Hindawi Publishing Corporation
Journal of Nanomaterials
Volume 2016, Article ID 9605906, 11 pages
http://dx.doi.org/10.1155/2016/9605906

Research Article

Antibacterial Activity of Partially Oxidized Ag/Au Nanoparticles against the Oral Pathogen *Porphyromonas gingivalis* W83

Megan S. Holden,[1] Jason Black,[2] Ainsely Lewis,[2] Marie-Claire Boutrin,[3] Elvin Walemba,[4] Theodore S. Sabir,[5] Danilo S. Boskovic,[1,4] Aruni Wilson,[3] Hansel M. Fletcher,[3] and Christopher C. Perry[1]

[1]*Division of Biochemistry, Loma Linda University School of Medicine, Loma Linda, CA 92350, USA*
[2]*Northern Caribbean University, Manchester, Jamaica*
[3]*Division of Microbiology and Molecular Genetics, Loma Linda University School of Medicine, Loma Linda, CA 92350, USA*
[4]*Department of Earth and Biological Sciences, Loma Linda University School of Medicine, Loma Linda, CA 92350, USA*
[5]*College of Arts and Sciences, Faulkner University, Montgomery, AL 36109, USA*

Correspondence should be addressed to Christopher C. Perry; chperry@llu.edu

Received 24 September 2015; Accepted 26 January 2016

Academic Editor: Nay Ming Huang

Advances in nanotechnology provide opportunities for the prevention and treatment of periodontal disease. While physicochemical properties of Ag containing nanoparticles (NPs) are known to influence the magnitude of their toxicity, it is thought that nanosilver can be made less toxic to eukaryotes by passivation of the NPs with a benign metal. Moreover, the addition of other noble metals to silver nanoparticles, in the alloy formulation, is known to alter the silver dissolution behavior. Thus, we synthesized glutathione capped Ag/Au alloy bimetallic nanoparticles (NPs) *via* the galvanic replacement reaction between maltose coated Ag NPs and chloroauric acid ($HAuCl_4$) in 5% aqueous triblock F127 copolymer solution. We then compared the antibacterial activity of the Ag/Au NPs to pure Ag NPs on *Porphyromonas gingivalis* W83, a key pathogen in the development of periodontal disease. Only partially oxidized glutathione capped Ag and Ag/Au (Au : Ag ≈ 0.2) NPs inhibited the planktonic growth of *P. gingivalis* W83. This effect was enhanced in the presence of hydrogen peroxide, which simulates the oxidative stress environment in the periodontal pocket during chronic inflammation.

1. Introduction

Advances in nanotechnology provide opportunities for the fabrication of silver containing nanoparticles (NPs) that can act as antimicrobial agents [1]. These NPs offer advantages over traditional therapies including reduced toxicity, lower cost, weak ability of bacteria to develop resistance [2, 3], and the ability to inhibit biofilms [4–6]. Additionally, silver (Ag) NPs [7] were shown to be less toxic to humans than traditional antibacterial Ag compounds such as silver nitrate [8] and silver sulfadiazine [9]. The physicochemical properties (size, shape, composition, and surface chemistry) of Ag NPs are known to influence the magnitude of their toxicity by affecting the degree of dissolution and delivery of silver ions [10–12]. Thus, the manipulation of these properties presents potential avenues for useful antibacterial preparations.

A potential application of Ag nanomaterials is to supplement or replace conventional antibiotic treatments for periodontal disease. Periodontal disease is characterized by tissue damage and subsequent tooth loss. Moreover, the most common form of periodontal disease, chronic periodontitis, occurs in nearly half of the Americans over the age of 30 [13, 14]. Infection-induced periodontal disease is acknowledged to be polymicrobial in nature [15, 16] with the key pathogens, "the red complex," being anaerobes [17, 18]. One of these "key pathogens" is *Porphyromonas gingivalis*, a black-pigmented gram-negative anaerobe. This anaerobe resides within the low oxygen environment of the periodontal pocket [19] and

is implicated in manipulating the host immune system and bringing about changes in the oral microbial community that contribute to chronic inflammation and tissue damage [20]. Chronic inflammation results in an excess of oxidative species such as hydrogen peroxide (H_2O_2), superoxide radicals ($^{\bullet}O_2^-$), and hydroxyl radicals ($^{\bullet}OH$). Continuously elevated levels of oxidative species are known to cause oxidative damage to tissues and is termed "oxidative stress" [21, 22]. Moreover, the chronic inflammation associated with periodontal diseases is also a risk factor for cardiovascular diseases [23], diabetes [24], and rheumatoid arthritis [25, 26]. Thus, targeting pathogens in "the red complex" could be beneficial for the treatment of periodontal disease and for reducing the risk of occurrence of secondary diseases that are associated with it.

Conventional antibiotic therapeutic strategies against periodontal pathogens suffer from microbial resistance [27–29] and problems maintaining a functional effective dose within the periodontal pocket [29, 30]. Therefore, there is a need for antimicrobials that are effective against anaerobes, can remove mature oral biofilms, carry low risk of resistance building in bacteria, and have minimal or no side effects. Several studies have investigated the antibacterial effects of Ag NPs. The proposed mechanisms of Ag NP-related toxicity include membrane damage, reactive oxygen species-based lipid and DNA damage, Ag^+ ion-based DNA damage, and interaction of Ag^+ ions with intracellular proteins [31–33]. Nonetheless, the antibacterial mode of action is dependent upon the aqueous solution environment [34, 35] and the composition of the nanomaterial [36]. While Ag NPs are strongly antibacterial towards aerobes, such effects are greatly reduced or lost in anaerobic environments. Lok and coworkers showed that partially oxidized silver nanoparticles had antibacterial activity but zero-valent nanoparticles did not [37]. Alvarez and coworkers found that exposing Ag NPs to oxygen significantly enhanced NP toxicity towards *E. coli* under anaerobic conditions in a concentration dependent manner [10, 38]. Moreover, Ag NPs synthesized and tested under anaerobic conditions lacked antibacterial activity [10]. Lu and coworkers, conversely, reported that Ag NPs had some antibacterial activity against oral anaerobic bacteria [7]. However, they noted that the Ag NPs were more toxic to aerobic bacteria than to anaerobic bacteria and concluded that the enhanced toxicity under aerobic conditions was from oxygen-induced dissolution of silver ions (Ag^+) from the Ag NPs [7]. In the case of eukaryotic cells, Prasad and coworkers found similar *in vitro* cellular stress responses after Ag NP and $AgNO_3$ exposures and concluded that the oxidative stress and inflammation effects of Ag NPs are caused by Ag^+ cytotoxicity [39].

It was further reported that the addition of other noble metals to silver nanoparticles, in the alloy formulation, is known to alter the silver dissolution behavior and reduce their overall toxicity towards eukaryotes [40]. Here we document a facile synthesis of Ag/Au biocompatible bimetallic NPs *via* the galvanic replacement reaction between maltose coated Ag NPs and chloroauric acid ($HAuCl_4$) in 5% aqueous triblock F127 copolymer solution. This provides an alternative "green" approach to synthesize biocompatible Ag/Au NPs that are less cytotoxic toward eukaryotic cells than Ag NPs [41, 42]. The nanoparticles were capped with glutathione. *In vivo* studies have shown that glutathione capped gold nanoparticles do not produce morbidity and have increased biocompatibility, higher cellular uptake, and longer circulation times than polyethylene glycol (PEG) [43].

We present results showing the antibacterial effectiveness of silver and silver/gold bimetallic nanoparticles against the anaerobic oral pathogen *P. gingivalis* W83. Since oxidative stress is one of the main causes of the inflammatory environment found in the periodontal pocket, its physiological level has been simulated by the addition of hydrogen peroxide *in vitro* [21, 22, 44–48]. So in this study we also determined the effects of (0.1–0.25 mM) hydrogen peroxide induced stress on the antibacterial activity of Ag and Ag/Au nanoparticles against *P. gingivalis* W83.

2. Materials and Methods

2.1. Materials. Ammonium hydroxide (28–30%), D-maltose (≥99%), NaOH (≥98%), silver nitrate (≥99%), gold(III) chloride hydrate ($HAuCl_4 \cdot 3H_2O$; 99.999% trace metals basis), Pluronic F127 ($EO_{100}PO_{65}EO_{100}$, MW ≈ 12500; batch number 119K0073), and reduced glutathione were used as received (Sigma-Aldrich, Milwaukee, WI). Milli-Q water (Millipore) was used in all experiments.

2.2. Synthesis and Characterization of Nanoparticles. Nanoparticles were prepared in an anaerobic chamber (37°C) or aerobically (on the bench) at room temperature. Aerobically prepared NPs were stored under anaerobic conditions within 30 minutes of synthesis until use. Both Ag and Ag/Au NPs were characterized by atomic force (AFM) and electron microscopies as well as UV-vis, Fourier transform infrared spectroscopy (FTIR), and dynamic light scattering (DLS) (Supporting Information Section A in Supplementary Material available online at http://dx.doi.org/10.1155/2016/9605906). Maltose coated Ag NPs were prepared via the reduction of $AgNO_3$ by maltose in an alkaline environment [49–51]. Bimetallic Ag/Au NPs were synthesized *via* the galvanic replacement reaction between maltose coated Ag NP seeds and $HAuCl_4$ [51].

The concentrations of the Ag NPs were determined by interpolating the extinction coefficients. These functions are as follows: $\lambda_{max}(x) = a + b \cdot x^2$ ($a = 397$ nm; $b = 9.58 \times 10^{-3}$ nm^{-1}). The $\varepsilon(\lambda_{max})$ in the size range 10–30 nm: $y(x) = y_0 + A \cdot \exp(R \cdot x)$ ($y_0 = -1.43 \times 10^9$, $A = 6.984 \times 10^8$, and $R = 0.104$), and between 30 and 100 nm: $y(x) = y_0 + k \cdot x$ ($y_0 = -4.709 \times 10^{10}$, $k = 2.017 \times 10^9$), where x is NP diameter [52]. The synthesized Ag NPs (≈3 nM, ~10^{12} particles/mL), in 5% (w/v) F127, were diluted to an optical density of 12 at ≈400 nm by further addition of 5% Pluronic F127. Bimetallic NPs of different Ag : Au ratios were synthesized by adding $HAuCl_4$ (0.2 M, 1 μL or 0.1 M, 1–6 μL) to 1 mL of Ag NP seed solution. The reaction was allowed to run for 30 minutes (the color change was instantaneous on thorough mixing) and the Au : Ag ratio was interpolated from the wavelength maxima

and verified by electron-dispersive X-ray spectroscopy (EDS) (Figure S1). Material characterization of Ag/Au bimetallic NPs by transmission electron microscopy (TEM) is described elsewhere [51].

Silver and Ag/Au NPs were capped with glutathione by two methods. In method I, nanoparticles are capped with glutathione by adding 10 μL of 10 mM glutathione (final concentration 0.1 mM) to 990 μL of as-prepared Ag/Au nanoparticle solution. The reaction is allowed to run for 30 minutes and the resulting particles are diluted to $OD_{\lambda max} = 1$ in 5% Pluronic F127 and stored anaerobically. In method II, glutathione (0.1 mM, 10 μL) was added to Ag and Ag/Au NPs in 1 mL 5% w/v F127 and incubated for ~12 hours prior to use. All NPs were stored under anaerobic conditions until use. To evaluate colloidal stability, 10 μL of 10 mM glutathione (final concentration 0.1 mM) was added to 990 μL of as-prepared nanoparticle solutions and the reaction was allowed to run for 30 minutes. The NPs were centrifuged and suspended in 5% aqueous F127 solution. These NPs were diluted 10-fold in 10 mM phosphate buffer saline solution (138 mM NaCl, 3 mM KCl). The extent of NP aggregation was assessed by DLS.

2.3. Bacterial Strain and Culture Conditions. *P. gingivalis* W83 was grown in cysteine-free Brain Heart Infusion (BHI) broth (Difco Laboratories, Detroit, MI) supplemented with yeast extract (5 mg/mL), hemin (5 μg/mL), and vitamin K (0.5 μg/mL) as per standard protocol for hydrogen peroxide stress experiments [44–48]. All cultures were incubated at 37°C unless otherwise stated. The *P. gingivalis* W83 strain was maintained in an anaerobic chamber (Coy Manufacturing, Ann Arbor, MI) in 10% H_2, 10% CO_2, and 80% N_2. Growth rates for *P. gingivalis* W83 were determined spectrophotometrically (optical density at 600 nm) using a quartz cell with a 1 cm path length at 25°C.

2.4. NP Sensitivity and Survival Assays. Overnight cultures of *P. gingivalis* W83 were used to inoculate prewarmed (37°C) BHI broth to early log phase ($OD_{600\,nm} \approx 0.1$). These cultures were then split into equal aliquots (4.5–4.6 mL), incubated anaerobically at 37°C until $OD_{600\,nm} \approx 0.15$, and inoculated with either (a) 400 μL sterile water, (b) 500 μL stock NPs (0.03 nM final concentration), (c) 400 μL stock NPs that were previously adjusted to OD = 1 or 4 (0.04–0.14 nM final concentration), or (d) 400 μL 6.25 mM $AgNO_3$ (0.5 mM final concentration), to give a 5 mL final volume. Inoculation of the controls with 400 μL sterile water was done since the NP suspensions are aqueous. In separate experiments (data not shown), the growth of the bacteria in undiluted broth was comparable to inoculation with 400 μL sterile water, inoculation with 400 μL of 5% F127, and inoculation with 400 μL glutathione (0.1 mM final concentration). The final dilution of the NPs resulted in an acceptable scattering error contribution (5–10%) for the UV-vis absorbance ($OD_{\lambda max} < 0.1$).

For H_2O_2 sensitivity and survival assays, overnight cultures were used to inoculate prewarmed (37°C) BHI broth to early log phase ($OD_{600\,nm} \approx 0.1$). These cultures were then split into equal aliquots (4.5–4.6 mL), incubated anaerobically at 37°C until $OD_{600\,nm} \approx 0.20$, inoculated with anaerobically prepared NPs, and stressed with subinhibitory (0.1 mM) and inhibitory (0.25 mM) concentrations of H_2O_2 [47]. All cultures were further incubated at 37°C for 24 hours. Absorbance readings at 600 nm (Bio-Rad Laboratories, Hercules, CA) were taken at specific intervals to assess growth of cells. When W83 controls reached $OD_{600\,nm} = 0.6$–0.8, 1 mL of each sample was removed and 10^{-6} dilutions were made with prewarmed BHI broth. An aliquot (100 μL) of each dilution was spread onto prewarmed and reduced BHI agar plates. Colonies were enumerated after 10 days of anaerobic incubation at 37°C. The colony counts were obtained using imaging processing software (Image J).

2.5. Statistical Analysis. Statistical significance for growth curves at 24 hours was determined at $\alpha = 0.05$ using one-way analysis of variance (ANOVA) with Bonferroni's posttest. Significant differences in colony growth from the control were determined at $\alpha = 0.05$ using two-tailed nonpaired Student's t-test. All statistical analyses were performed using SPSS Statistics Version 22 (IBM SPSS Statistics, Chicago, IL). A $p \leq 0.05$ was considered to be significant.

3. Results and Discussion

Figure 1 shows characterization of Ag/Au NPs synthesized by adding $HAuCl_4$ (0.2 M, 1 μL) to 1 mL of Ag NP seed solution ($OD_{400\,nm} \approx 12$). Both synthesized Ag seeds and Ag/Au NPs have a single population with predominantly spherical shapes. Based on the AFM data, the relative heights of the Ag and Ag/Au NPs were determined to be 14 ± 2 and 17 ± 5 nm, respectively. Figures 1(c) and 1(d) are representative TEM images of the Ag seeds and Ag/Au bimetallic NPs, with mean diameters of 22 ± 3 and 16 ± 5 nm, respectively. The darker electron contrast in the Ag/Au NPs indicates heterogeneous electron scattering from the gold and silver. This suggests that the particles have extensive pitting and may have hollow interiors. More importantly, differences in electron contrast in the TEM image indicate that dissolution of Ag(0) and the deposition of Au are not uniform on the NP surface. Galvanic replacement reaction studies indicate that Au deposition preferentially occurs on high-energy {110} and {100} facets [53]. The deposition of Au onto the high-energy facets inhibits Ag oxidation, while the uncoated low energy {111} facets become sites for Ag dissolution in a self-seeding process [54]. This is ultimately responsible for the extensive pitting observed when the bimetallic NPs are prepared. Moreover, the TEM observation that the Ag/Au NPs possess smaller average diameter is indicative of an overall reduction in the number of atoms in the structure of the NPs from alloying at the interfacial regions [55].

Figure 1(e) shows the absorption spectra for Au, Ag, and Ag/Au alloy and a mixture of Ag and Au NPs. The monometallic dispersions of Ag and Au NPs possess localized surface plasmon resonance (LSPR) bands with peak maxima of ≈400 nm and ≈530 nm, respectively. The single LSPR band for the Ag/Au NPs is red shifted (≈428 nm) compared to Ag (≈400 nm) and indicates the formation of alloyed bimetallic NPs [56, 57]. If the NP dispersion had been a mixture of Ag and Au NPs, the LSPR band would be bimodal with

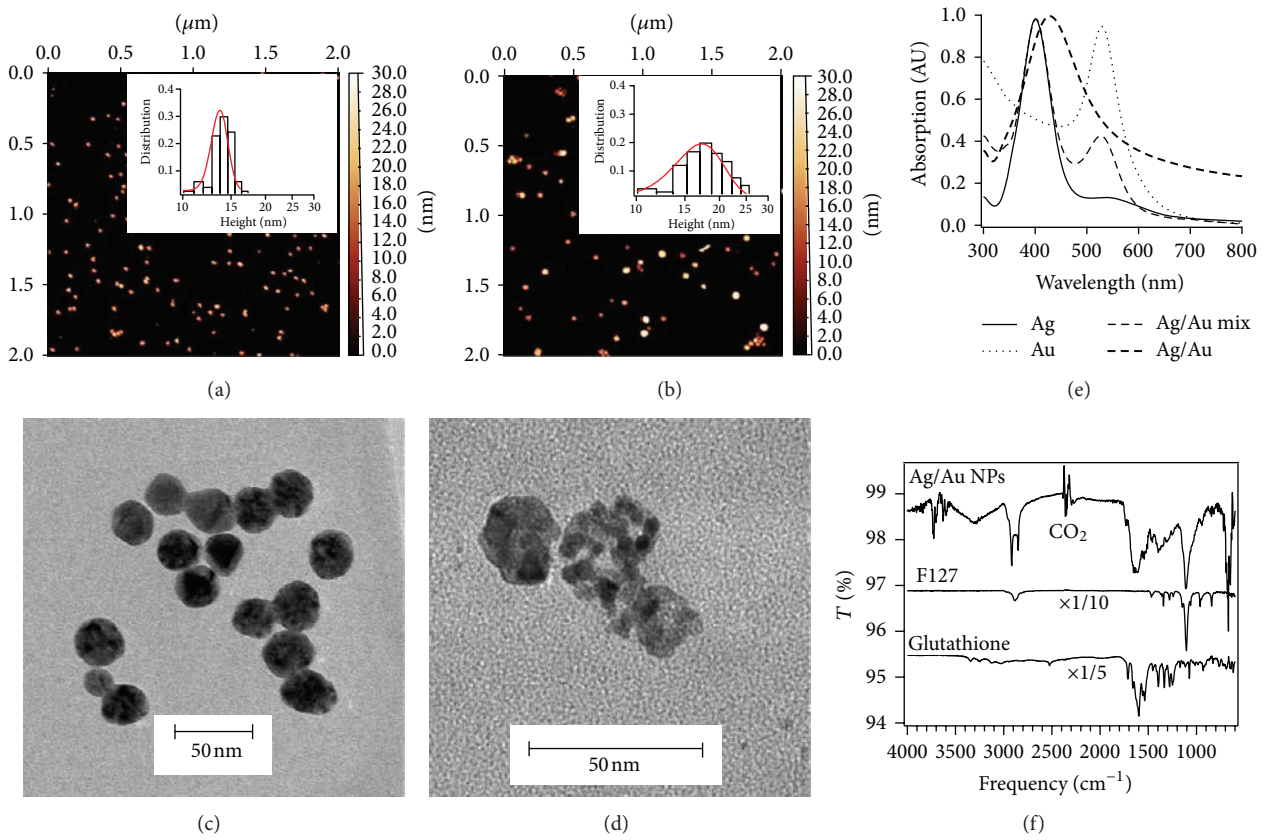

Figure 1: Materials characterization of Ag and Ag/Au nanoparticles. Atomic force microscopy images of (a) Ag (14 ± 2 nm; $N = 143$) and (b) Ag/Au (17 ± 5 nm; $N = 523$) nanoparticles with height distributions. Transmission electron microscopy images of (c) Ag and (d) Ag/Au nanoparticles. The nanoparticles were prepared by adding $HAuCl_4$ (0.2 M, 1 μL) to 1 mL of Ag NP seed solution ($OD_{400\,nm} = 12$). (e) UV-vis absorption spectra of Ag, Au, a mixture of Ag and Au, and Ag/Au nanoparticles normalized to their peak maxima. (f) Infrared spectra confirming glutathione chemisorption on the surface of Ag/Au NPs. Glutathione (0.1 mM, 10 μL) was added to Ag/Au nanoparticles in 1 mL 5% w/v F127 and left for ≈12 hours. The nanoparticles were washed by centrifugation (10000 ×g; 20 minutes) in water twice before analysis.

peaks corresponding to Ag and Au NPs, respectively. EDS analysis confirmed the incorporation of Au (Au : Ag ratio ≈ 0.2) (Figure S2). X-ray diffraction characterization showed 30% AgCl contamination on the formed bimetallic NPs when $HAuCl_4$ was added to the Ag NPs at 25°C, even after washing by centrifugation [51].

Thermodynamic analysis of bulk silver predicts that Ag(0) is not an equilibrium oxidation state in aqueous environments that are acidic or contain any significant amount of dissolved O_2 [58]. Under these conditions, Ag^+ is readily released from bulk silver:

$$4Ag\,(0) + O_2 \longrightarrow 2Ag_2O \quad (1)$$

$$2Ag_2O + 4H^+ \longrightarrow 4Ag^+ + 2H_2O \quad (2)$$

giving an overall stoichiometry of

$$2Ag_{(s)} + \frac{1}{2}O_2 + 2H^+{}_{(aq)} \longrightarrow 2Ag^+{}_{(aq)} + H_2O_{(l)}. \quad (3)$$

These conclusions also hold true for nanoscale silver [59]. Even though Ag(0) is thermodynamically unstable, the dissolution of Ag(0) to Ag^+ in Ag colloids is kinetically controlled. Silver ions are also produced during the galvanic replacement of silver by chloroauric acid ($HAuCl_4$) to form AgCl during the bimetallic NP synthesis:

$$3Ag_{(s)} + AuCl_4{}^-{}_{(aq)} \longrightarrow Au_{(s)} + 3AgCl_{(s)} + Cl^-{}_{(aq)}. \quad (4)$$

There is speciation of the silver ions, with partitioning between aqueous Ag^+ and surface-adsorbed AgCl ($AgCl_{(s)} \leftrightarrow Ag^+{}_{(aq)} + Cl^-{}_{(aq)}$), where the silver ions will be sequestered by sulfur (as thiols, e.g., cysteine groups in proteins) and other ligands in biological media [34, 38].

The synthesized Ag/Au NPs were capped with glutathione to increase the colloidal stability of the NPs in saline media (Figure 1(f)). Glutathione was chosen as a capping agent for several reasons. First, glutathione contains thiol groups which have high affinity for noble metal surfaces allowing for the chemisorption of glutathione onto the surface of the Ag/Au NPs [60]. Second, the pH-dependent charged functional groups promote water solubility and interact with biostructures [61, 62]. Lastly, this capping agent can be applied to as-prepared NPs and does not interfere with the antibacterial activity of colloidal Ag NPs [4, 63]. FTIR was used to confirm the chemisorption of glutathione on

the surface of the NPs (Figure 1(f)). There is one-to-one correspondence in the fingerprint region below 1700 cm^{-1} between crystalline and glutathione capped Ag/Au NPs with amide I and II bands being observed [64, 65]. Amide I bands between 1600 and 1700 cm^{-1} correspond to the stretching vibrations of the C=O and C-N groups. Amide II bands between 1510 and 1580 cm^{-1} correspond to the in-plane N-H bending, the C-N stretching, and the C-C stretching vibrations. We performed DLS colloidal stability studies with glutathione (0.1 mM) capped and uncapped Ag/Au NPs in 10 mM phosphate saline. The hydrodynamic diameters (~ 60 nm) of glutathione capped Ag/Au NPs were stable for at least 24 hours while the uncapped Ag/Au NPs aggregated after 1 hour (Figure S3). The zeta potentials were ≈−15 meV over the range of F127 capped Ag/Au NP Ag : Au ratios, decreasing to ≈−22 meV when capped with glutathione. The zeta potentials for maltose coated Ag (≈−20 meV) and glutathione capped bimetallic NPs are similar indicating that both will be colloidally stable in biological media.

Colloidal stability is also important for antibacterial activity. Bacterial growth over a 24 h period was assessed by measuring the absorbance of the cultures at 600 nm at specific time intervals. Control experiments with 0.1 mM glutathione demonstrate that it does not influence the growth of *P. gingivalis* W83 (Figure S4). Glutathione capped Ag/Au NPs prepared aerobically inhibited the growth of *P. gingivalis* W83 while the uncapped Ag/Au NPs showed no inhibition and precipitated out of solution when exposed to BHI broth overnight (Figure S5). Thus, colloidal stability is crucial for the antibacterial activity of Ag/Au alloy NPs under anaerobic conditions.

We prepared glutathione capped Ag and Ag/Au (Au : Ag = 0.10–2.2) NPs in the anaerobic chamber. *P. gingivalis* W83 was inoculated with these NPs (final concentration ≈ 0.03 nM) for 24 hours. The bacterial growth curves after 24 hours showed no statistical significance between NP treated and untreated bacteria (Figure 2). This result is consistent with previous reports that Ag NP antibacterial activity is from the Ag^+ ions released from partially oxidized silver [38, 66]. Figure 3 shows the growth curves of bacteria incubated with aerobically prepared NPs (final concentration ≈ 0.03 nM). *P. gingivalis* W83 was inoculated with Ag or glutathione capped Ag and Ag/Au (Au : Ag = 0.30 ± 0.05) NPs suspended in 5% aqueous F127. All NPs have similar (~25%) inhibition of growth after 24 hours, which is independent of surface coating. This result is consistent with studies showing a weak association of surface capping agents and the rate of Ag^+ ion release at constant particle core size [10].

Even though Ag NPs show strong antibacterial activity towards aerobes, they exhibit greatly reduced or no antibacterial activity when they are prepared anaerobically. The release of Ag^+ from the Ag_2O layer is facilitated by the bacterial proton motive force decreasing the local pH (Equation (3)) [67]. This hypothesis is supported by the data in Figures 2 and 3 demonstrating that partial silver oxidation was necessary for antibacterial activity. This suggests that the oxide layer is necessary for antibacterial activity rather than the surface AgCl, which is present in both aerobically and anaerobically

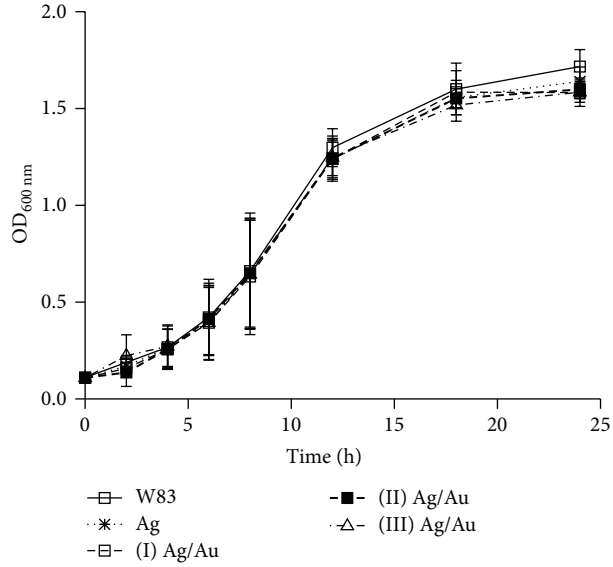

Figure 2: Growth curves of *P. gingivalis* W83 showing the antibacterial activities of anaerobically prepared nanoparticles. Bacterial growth over a 24-hour period was assessed by measuring the absorbance of cultures at 600 nm for specific intervals. *P. gingivalis* W83 was inoculated with anaerobically prepared (≈0.3 nM, 500 μL) glutathione capped Ag and Ag/Au ((I) Au : Ag = 0.10 ± 0.04; (II) Au : Ag = 0.30 ± 0.05; (III) Au : Ag = 2.2 ± 0.1) nanoparticles in 5 mL total volume. Glutathione capping was done using method II. Error bars represent the standard deviation of three experiments.

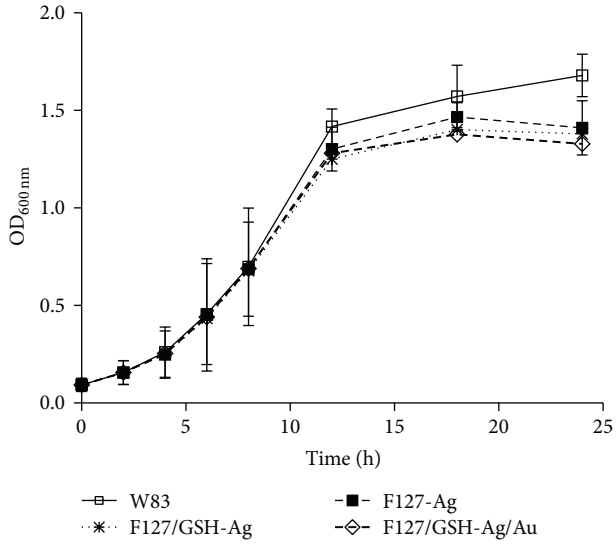

Figure 3: Growth curves of *P. gingivalis* W83 showing the antibacterial activities of aerobically prepared nanoparticles. Bacterial growth over a 24-hour period was assessed by measuring the absorbance of cultures at 600 nm for specific intervals. *P. gingivalis* W83 was inoculated with aerobically prepared Ag nanoparticles coated with F127 (≈0.3 nM, 500 μL) or glutathione capped (≈0.3 nM, 500 μL) and Ag/Au (Au : Ag = 0.30 ± 0.05; ≈0.3 nM, 500 μL) nanoparticles in 5 mL total volume. Glutathione capping was done using method II. Error bars represent the standard deviation of three experiments.

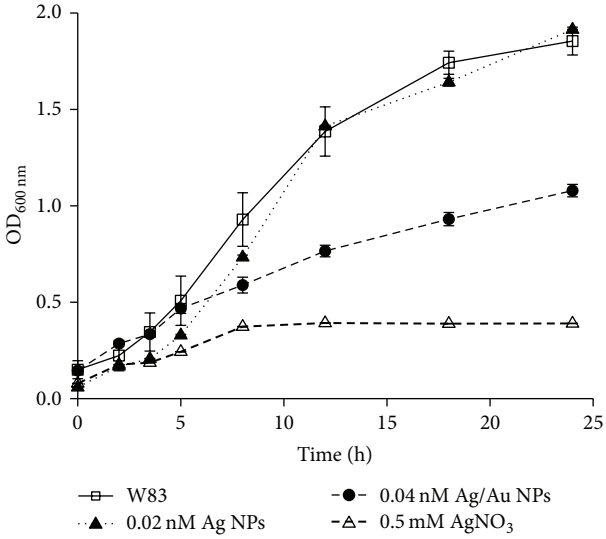

Figure 4: Growth curves of *P. gingivalis* W83 comparing the antibacterial activity of aerobically prepared nanoparticles with 0.5 mM $AgNO_3$. Bacterial growth over a 24-hour period was assessed by measuring the absorbance of cultures at 600 nm for specific intervals. *P. gingivalis* W83 ($OD_{600\,nm} \approx 0.15$) was challenged with water (400 μL), maltose coated Ag (≈0.2 nM, 400 μL; $OD_{\lambda max} = 1$) or glutathione capped Ag/Au (Au : Ag ≈ 0.2; ≈0.4 nM, 400 μL; $OD_{\lambda max} = 1$) nanoparticles, or 0.5 mM $AgNO_3$ (6.25 mM, 400 μL) in 5 mL total volume. Glutathione capping was done using method I. Error bars represent the standard deviation of three experiments.

prepared NPs. Thus, the release of Ag^+ from the Ag_2O layer may be primarily responsible for the antibacterial activity of Ag NPs [7].

Figure 4 shows growth curves at higher concentrations of aerobically prepared glutathione capped Ag/Au NPs (Au : Ag ≈ 0.2; 0.04 nM final concentration). In this case, maltose capped Ag (≈0.02 nM final concentration) and glutathione capped Ag/Au NPs were added from $OD_{\lambda max} = 1$ stock solutions. Maltose capped Ag NPs were used to determine if their oxidation is the main determinant in the antibacterial activity of Ag/Au NPs. The growth curve of *P. gingivalis* W83 is shown for comparison. Aerobically prepared Ag/Au NPs as well as 0.5 mM $AgNO_3$ exhibited antibacterial activity against *P. gingivalis* W83 at 12 ($p < 0.01$) and 24 ($p < 0.01$) hours. Below 0.1 mM $AgNO_3$, the bacteria recover from the inhibitory effects of Ag^+ after 24 hours (Figure S6). Indeed, a closer examination of Figure 4 reveals that maltose capped Ag NPs prepared aerobically have an inhibitory effect on bacterial growth during the early exponential growth phase (4–12 hours).

The sensitivity of *P. gingivalis* W83 was also assessed using colony count assays when cultures were at OD ≈ 0.5 (after six hours of treatment; $\approx 8 \times 10^8$ CFU/mL W83 control) (Table 1). The glutathione capped $OD_{\lambda max} = 1$ (≈0.04 nM) and $OD_{\lambda max} = 4$ (≈0.14 nM) Ag/Au NPs (Au : Ag ≈ 0.2) decreased *P. gingivalis* W83 survival by approximately $\log_{10}(0.4)$ CFU/mL (≈3-fold decrease) and $\log_{10}(1.3)$ CFU/mL (≈20-fold decrease), respectively ($p < 0.01$). Collectively, these data indicate that the Ag/Au NPs (>0.04 nM) have

Table 1: Antibacterial activity on *P. gingivalis* W83 determined by colony forming units.

	$\log_{10}$ (CFU/mL)	[a]$\Delta\log_{10}$ (CFU/mL)
W83	9.4	0
Maltose –Ag NPs	9.5	+0.1
GSH–Ag/Au NPs (0.04 nM)	9.0	−0.4
GSH–Ag/Au NPs (0.14 nM)	8.1	−1.3
0.25 mM H_2O_2	7.9	−1.5
0.25 mM H_2O_2 + Ag/Au (0.04 nM)	7.8	−1.6
BHI	0.0	0

[a]Negative sign: log CFU/mL decrease.

comparable antibacterial activities to 0.5 mM $AgNO_3$. The preparation process for Ag/Au NPs involves the Ag NPs being centrifuged on the bench to remove the excess reagents and suspended in 5% w/v F127 aqueous solution prior to adding Au(III). During this process to synthesize Ag/Au NPs, further oxidation of the silver occurs and this enhances its antibacterial activity.

Because it is well established that periodontal disease is associated with inflammation [21, 22], we assessed the influence of hydrogen peroxide on the antibacterial activities of the NPs (Figures 5 and 6). We grew *P. gingivalis* W83 culture overnight. Prewarmed BHI broth was inoculated using the overnight culture to an OD ≈ 0.1. Bacteria were grown to OD ≈ 2 and then split into equal aliquots and inoculated with anaerobically prepared NPs and stressed with subinhibitory (0.1 mM) or inhibitory (0.25 mM) concentrations of H_2O_2 [47]. All cultures were further incubated at 37°C for 12 or 24 h (Figure 5). We observed that the addition of anaerobically prepared NPs to *P. gingivalis* W83 exposed to H_2O_2 did not further inhibit bacterial growth. In contrast, aerobically prepared Ag and Ag/Au NPs in combination with 0.25 mM of H_2O_2 completely inhibited bacterial growth (Figure 6).

To further assess the influence of H_2O_2 concentration (0.01–0.25 mM) on aerobically prepared NP antibacterial activity, we compared bacterial growth at 12 and 24 hours (Figure S7). Overnight cultures of *P. gingivalis* W83 were incubated anaerobically at 37°C until $OD_{600\,nm} \approx 0.1$ and inoculated with treatments of water, maltose capped Ag (≈0.02 nM), or glutathione capped Ag/Au (Au : Ag ≈ 0.2) nanoparticles. When $OD_{600\,nm}$ of the *P. gingivalis* W83 control was ≈ 0.2, H_2O_2 was added. Only at 0.25 mM H_2O_2 were there synergistic growth inhibition effects on *P. gingivalis* W83 with $AgNO_3$, Ag, and Ag/Au NPs (Figures S7A, S7C). To correlate the effect of H_2O_2 and NPs, the absorbance measurements were normalized against the corresponding values in the absence of H_2O_2 after 12 and 24 hours (Figures S7B, S7D). We note that $AgNO_3$ has the best antibacterial activity after 24 hours. A likely explanation is that the molar excess of H_2O_2 oxidizes the *in situ* generated Ag NPs, made in the reducing environment of the growth media, back to Ag^+.

As Ag NPs are capable of disrupting microbial cell walls and bacterial membranes [68, 69], we used AFM to investigate the action of aerobically prepared glutathione capped

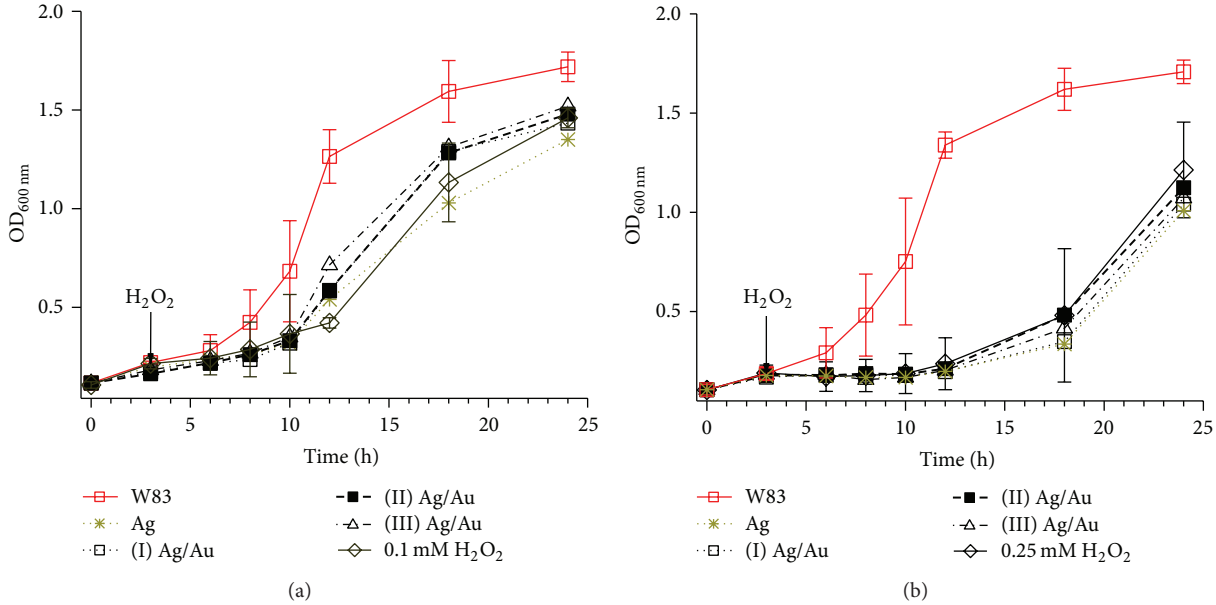

FIGURE 5: Growth curves of *P. gingivalis* W83 stressed with (a) 0.1 or (b) 0.25 mM H_2O_2 in the presence of anaerobically prepared Ag and Ag/Au nanoparticles. Bacterial growth over a 24-hour period was assessed by measuring the absorbance of cultures at 600 nm for specific intervals. Bacteria were inoculated with glutathione (≈0.3 nM, 500 μL) capped Ag and Ag/Au ((I) Au : Ag = 0.10±0.04; (II) Au : Ag = 0.30±0.05; (III) Au : Ag = 2.2 ± 0.1) nanoparticles in 5 mL total volume. Glutathione capping was done by method II. Hydrogen peroxide was added when $OD_{600\,nm}$ of W83 control was ≈0.2. Error bars represent the standard deviation of three experiments.

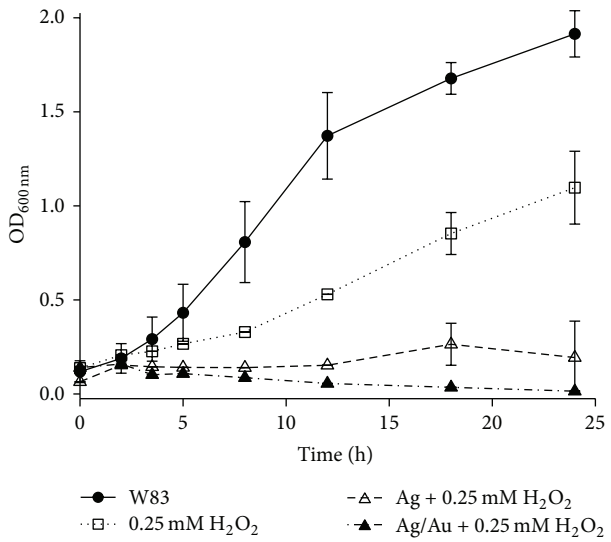

FIGURE 6: Growth curves of *P. gingivalis* W83 stressed with 0.25 mM H_2O_2 in the presence of aerobically prepared Ag and Ag/Au nanoparticles. Bacterial growth over a 24-hour period was assessed by measuring the absorbance of cultures at 600 nm for specific intervals. Actively growing *P. gingivalis* W83 (OD_{600} ≈ 0.2) was challenged with maltose coated Ag (≈0.2 nM, 400 μL; $OD_{\lambda max}$ = 1) or glutathione capped Ag/Au (Au : Ag ≈ 0.2; ≈0.4 nM, 400 μL; $OD_{\lambda max}$ = 1) nanoparticles in 5 mL total volume. Glutathione capping was done by method II. Hydrogen peroxide was added when $OD_{600\,nm}$ of W83 control was ≈0.2. Error bars represent the standard deviation of three experiments.

Ag/Au NPs on the surface structure of *P. gingivalis* W83. The AFM images of untreated *P. gingivalis* W83 reveal intact cells with undamaged membranes and typical dimensions of ~1 μm (Figure 7(a)). In contrast, AFM images of *P. gingivalis* W83 exposed to 0.5 mM $AgNO_3$ for ≈3 hours resulted in cell lysis and death (Figure 7(b)). The bright contrast in the image is assigned to Ag NPs formed from the reduction of Ag^+ ions. Broth containing *P. gingivalis* W83 will be strongly reducing, containing volatile sulfur compounds including hydrogen sulfide, methyl mercaptan (methanethiol), and dimethyl sulfide, where methyl mercaptan is believed to play a role in the pathogenicity of *P. gingivalis* W83 [70]. Thus, it is likely that Ag^+ ions are reduced by thiols such as methyl mercaptan:

$$2Ag^+_{(aq)} + 2CH_3SH_{(aq)} \longrightarrow CH_3SSCH_{3(aq)} + 2H^+_{(aq)} + 2Ag_{(s)}, \quad (5)$$

which have lower standard electrode potentials than silver [71]. Hydrogen peroxide, like silver nitrate, will also cause significant membrane damage (Figure 7(c)). AFM images of *P. gingivalis* W83 exposed to glutathione capped Ag/Au NPs for ≈10 min are similar to untreated bacteria and display no signs of structural damage (Figure 7(d)). When *P. gingivalis* W83 was exposed to glutathione capped Ag/Au NPs for ≈5 hours, AFM images show that a majority of the bacterial membranes are completely disrupted and that intracellular material is leaking out (Figure 7(e)). This indicates that

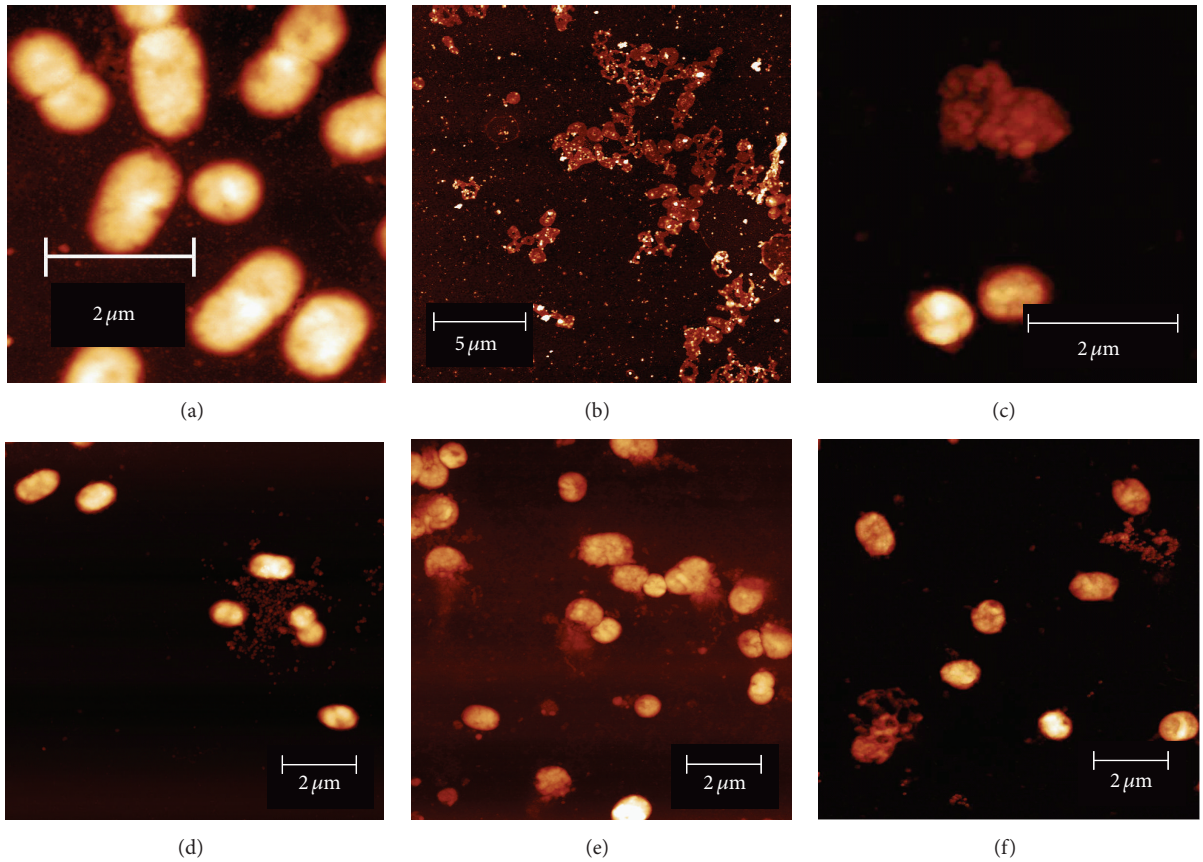

Figure 7: Representative atomic force microscopy height images of *P. gingivalis* W83 exposed to aerobically prepared Ag/Au nanoparticles. (a) Cells dividing in the exponential growth phase with undamaged membranes and typical dimensions (~$1 \times 1\,\mu m^2$). (b) *P. gingivalis* W83 exposed to 0.5 mM $AgNO_3$ for ≈3 hours (corresponding to OD ≈ 0.5 in W83 control growth phase) revealed significant bacterial lysis and membrane disruption. (c) *P. gingivalis* W83 exposed to 0.25 mM H_2O_2 showing bacterial lysis. (d) *P. gingivalis* W83 exposed to glutathione capped Ag/Au nanoparticles for ≈10 min is similar to untreated bacteria and displays no signs of structural damage. (e) When *P. gingivalis* W83 is exposed to glutathione capped Ag/Au nanoparticles for ≈5 hours the majority of the bacterial membranes are completely disrupted with intracellular material leaking out. (f) *P. gingivalis* W83 exposed to glutathione capped Ag/Au nanoparticles in the presence of 0.25 mM H_2O_2.

Ag/Au NP inhibition acts in a time-dependent manner. Complete membrane disruption is achieved in the presence of both 0.25 mM hydrogen peroxide and Ag/Au NPs (Figure 7(f)).

4. Conclusions

We describe a facile, economic, and environmentally benign method for the synthesis of glutathione capped Ag/Au bimetallic NPs. The synthesized NPs of Au : Ag ratio ≈ 0.2 capped with glutathione were colloidally stable in saline solution for at least 24 hours. The aerobically prepared glutathione capped Ag and Ag/Au (Au : Ag ratio ≈ 0.2) NPs have similar antibacterial activities against the anaerobic oral pathogen *P. gingivalis*. Moreover, the antibacterial activity of aerobically prepared NPs is enhanced in the presence of hydrogen peroxide. These data support the idea that partially oxidized silver with subsequent Ag^+ ion release from the Ag_2O overlayer is necessary for antibacterial activity [10, 37, 38]. There are compelling reasons for using Ag/Au bimetallic NPs. First, as a reservoir for Ag^+, the Ag/Au NPs stored in aqueous F127 copolymer solutions are more amenable for long-term storage. Second, Ag/Au NPs have the potential of providing a larger antimicrobial therapeutic window whilst minimizing acute toxicity to host eukaryotic cells. As a future direction, *in vitro* and *in vivo* cytotoxicity studies are needed to quantify the efficiency and toxicity of these biocompatible Ag/Au NPs.

Disclosure

Current address of Ainsely Lewis is Trent University, Peterborough, Ontario, Canada.

Conflict of Interests

The authors declare no conflict of interests with respect to the study, authorship, and publication of this paper.

Acknowledgments

This work was supported in part by Loma Linda University and NIH Grants (DE013664, DE019730, DE022508, and DE025852) from NIDCR (to Hansel M. Fletcher). The authors acknowledge the assistance provided by Drs. Henry and Roy, their technical assistance and editing of the paper. Access to the TEM was provided by the Central Facility for Advanced Microscopy and Microanalysis (CFAMM) at the University of California Riverside (UCR).

References

[1] S. Srinivasan, P. T. Kumar, S. V. Nair, S. V. Nair, K. P. Chennazhi, and R. Jayakumar, "Antibacterial and bioactive α- and β-chitin hydrogel/nanobioactive glass ceramic/nano silver composite scaffolds for periodontal regeneration," *Journal of Biomedical Nanotechnology*, vol. 9, no. 11, pp. 1803–1816, 2013.

[2] S. Pal, Y. K. Tak, and J. M. Song, "Does the antibacterial activity of silver nanoparticles depend on the shape of the nanoparticle? A study of the gram-negative bacterium *Escherichia coli*," *Applied and Environmental Microbiology*, vol. 73, no. 6, pp. 1712–1720, 2007.

[3] E. Weir, A. Lawlor, A. Whelan, and F. Regan, "The use of nanoparticles in anti-microbial materials and their characterization," *Analyst*, vol. 133, no. 7, pp. 835–845, 2008.

[4] E. Amato, Y. A. Diaz-Fernandez, A. Taglietti et al., "Synthesis, characterization and antibacterial activity against gram positive and gram negative bacteria of biomimetically coated silver nanoparticles," *Langmuir*, vol. 27, no. 15, pp. 9165–9173, 2011.

[5] I. Sondi and B. Salopek-Sondi, "Silver nanoparticles as antimicrobial agent: a case study on *E. coli* as a model for Gram-negative bacteria," *Journal of Colloid and Interface Science*, vol. 275, no. 1, pp. 177–182, 2004.

[6] F. Martínez-Gutierrez, E. P. Thi, J. M. Silverman et al., "Antibacterial activity, inflammatory response, coagulation and cytotoxicity effects of silver nanoparticles," *Nanomedicine: Nanotechnology, Biology, and Medicine*, vol. 8, no. 3, pp. 328–336, 2012.

[7] Z. Lu, K. Rong, J. Li, H. Yang, and R. Chen, "Size-dependent antibacterial activities of silver nanoparticles against oral anaerobic pathogenic bacteria," *Journal of Materials Science: Materials in Medicine*, vol. 24, no. 6, pp. 1465–1471, 2013.

[8] P. Spacciapoli, D. Buxton, D. Rothstein, and P. Friden, "Antimicrobial activity of silver nitrate against periodontal pathogens," *Journal of Periodontal Research*, vol. 36, no. 2, pp. 108–113, 2001.

[9] O. Brandt, M. Mildner, A. E. Egger et al., "Nanoscalic silver possesses broad-spectrum antimicrobial activities and exhibits fewer toxicological side effects than silver sulfadiazine," *Nanomedicine: Nanotechnology, Biology, and Medicine*, vol. 8, no. 4, pp. 478–488, 2012.

[10] Z.-M. Xiu, Q.-B. Zhang, H. L. Puppala, V. L. Colvin, and P. J. J. Alvarez, "Negligible particle-specific antibacterial activity of silver nanoparticles," *Nano Letters*, vol. 12, no. 8, pp. 4271–4275, 2012.

[11] M. N. Martin, A. J. Allen, R. I. Maccuspie, and V. A. Hackley, "Dissolution, agglomerate morphology, and stability limits of protein-coated silver nanoparticles," *Langmuir*, vol. 30, no. 38, pp. 11442–11452, 2014.

[12] T. S. Peretyazhko, Q. Zhang, and V. L. Colvin, "Size-controlled dissolution of silver nanoparticles at neutral and acidic pH conditions: kinetics and size changes," *Environmental Science and Technology*, vol. 48, no. 20, pp. 11954–11961, 2014.

[13] B. L. Pihlstrom, B. S. Michalowicz, and N. W. Johnson, "Periodontal diseases," *The Lancet*, vol. 366, no. 9499, pp. 1809–1820, 2005.

[14] P. I. Eke, B. A. Dye, L. Wei, G. O. Thornton-Evans, and R. J. Genco, "Prevalence of periodontitis in adults in the united states: 2009 and 2010," *Journal of Dental Research*, vol. 91, no. 10, pp. 914–920, 2012.

[15] R. P. Darveau, "Periodontitis: a polymicrobial disruption of host homeostasis," *Nature Reviews Microbiology*, vol. 8, no. 7, pp. 481–490, 2010.

[16] S. S. Socransky, A. D. Haffajee, M. A. Cugini, C. Smith, and R. L. Kent Jr., "Microbial complexes in subgingival plaque," *Journal of Clinical Periodontology*, vol. 25, no. 2, pp. 134–144, 1998.

[17] G. Hajishengallis and R. J. Lamont, "Beyond the red complex and into more complexity: the polymicrobial synergy and dysbiosis (PSD) model of periodontal disease etiology," *Molecular Oral Microbiology*, vol. 27, no. 6, pp. 409–419, 2012.

[18] G. Hajishengallis, S. Liang, M. A. Payne et al., "Low-abundance biofilm species orchestrates inflammatory periodontal disease through the commensal microbiota and complement," *Cell Host & Microbe*, vol. 10, no. 5, pp. 497–506, 2011.

[19] G. R. Mettraux, F. A. Gusberti, and H. Graf, "Oxygen tension (pO_2) in untreated human periodontal pockets," *Journal of Periodontology*, vol. 55, no. 9, pp. 516–521, 1984.

[20] R. P. Darveau, G. Hajishengallis, and M. A. Curtis, "Porphyromonas gingivalis as a potential community activist for disease," *Journal of Dental Research*, vol. 91, no. 9, pp. 816–820, 2012.

[21] L. G. Henry, M.-C. Boutrin, A. W. Aruni, A. Robles, A. Ximinies, and H. M. Fletcher, "Life in a diverse oral community—strategies for oxidative stress survival," *Journal of Oral Biosciences*, vol. 56, no. 2, pp. 63–71, 2014.

[22] L. G. Henry, R. M. E. McKenzie, A. Robles, and H. M. Fletcher, "Oxidative stress resistance in *Porphyromonas gingivalis*," *Future Microbiology*, vol. 7, no. 4, pp. 497–512, 2012.

[23] R. J. Genco and T. E. Van Dyke, "Reducing the risk of CVD in patients with periodontitis," *Nature Reviews Cardiology*, vol. 7, no. 9, pp. 479–480, 2010.

[24] E. Lalla and P. N. Papapanou, "Diabetes mellitus and periodontitis: a tale of two common interrelated diseases," *Nature Reviews Endocrinology*, vol. 7, no. 12, pp. 738–748, 2011.

[25] S. Kaur, S. White, and P. M. Bartold, "Periodontal disease and rheumatoid arthritis: a systematic review," *Journal of Dental Research*, vol. 92, no. 5, pp. 399–408, 2013.

[26] C. O. Bingham III and M. Moni, "Periodontal disease and rheumatoid arthritis: the evidence accumulates for complex pathobiologic interactions," *Current Opinion in Rheumatology*, vol. 25, no. 3, pp. 345–353, 2013.

[27] A. Mombelli, B. Schmid, A. Rutar, and N. P. Lang, "Persistence patterns of *Porphyromonas gingivalis*, *Prevotella intermedia/nigrescens*, and *Actinobacillus actinomycetemcomitans* after mechanical therapy of periodontal disease," *Journal of Periodontology*, vol. 71, no. 1, pp. 14–21, 2000.

[28] J. Sandros, P. Papapanou, and G. Dahlén, "*Porphyromonas gingivalis* invades oral epithelial cells in vitro," *Journal of Periodontal Research*, vol. 28, no. 3, pp. 219–226, 1993.

[29] American Academy of Pediatric Dentistry, "Treatment of plaque-induced gingivitis, chronic periodontitis, and other clinical conditions," *Pediatric Dentistry*, vol. 27, no. 7, supplement, pp. 202–211, 2006.

[30] "Treatment of plaque-induced gingivitis, chronic periodontitis, and other clinical conditions," *Journal of Periodontology*, vol. 72, no. 12, pp. 1790–1800, 2001.

[31] L. Rizzello and P. P. Pompa, "Nanosilver-based antibacterial drugs and devices: mechanisms, methodological drawbacks, and guidelines," *Chemical Society Reviews*, vol. 43, no. 5, pp. 1501–1518, 2014.

[32] B. Reidy, A. Haase, A. Luch, K. A. Dawson, and I. Lynch, "Mechanisms of silver nanoparticle release, transformation and toxicity: a critical review of current knowledge and recommendations for future studies and applications," *Materials*, vol. 6, no. 6, pp. 2295–2350, 2013.

[33] S. Eckhardt, P. S. Brunetto, J. Gagnon, M. Priebe, B. Giese, and K. M. Fromm, "Nanobio silver: its interactions with peptides and bacteria, and its uses in medicine," *Chemical Reviews*, vol. 113, no. 7, pp. 4708–4754, 2013.

[34] C. Levard, E. M. Hotze, G. V. Lowry, and G. E. Brown, "Environmental transformations of silver nanoparticles: impact on stability and toxicity," *Environmental Science & Technology*, vol. 46, no. 13, pp. 6900–6914, 2012.

[35] A. P. Gondikas, A. Morris, B. C. Reinsch, S. M. Marinakos, G. V. Lowry, and H. Hsu-Kim, "Cysteine-induced modifications of zero-valent silver nanomaterials: implications for particle surface chemistry, aggregation, dissolution, and silver speciation," *Environmental Science & Technology*, vol. 46, no. 13, pp. 7037–7045, 2012.

[36] M. Banerjee, S. Sharma, A. Chattopadhyay, and S. S. Ghosh, "Enhanced antibacterial activity of bimetallic gold-silver core-shell nanoparticles at low silver concentration," *Nanoscale*, vol. 3, no. 12, pp. 5120–5125, 2011.

[37] C.-N. Lok, C.-M. Ho, R. Chen et al., "Silver nanoparticles: partial oxidation and antibacterial activities," *Journal of Biological Inorganic Chemistry*, vol. 12, no. 4, pp. 527–534, 2007.

[38] Z.-M. Xiu, J. Ma, and P. J. J. Alvarez, "Differential effect of common ligands and molecular oxygen on antimicrobial activity of silver nanoparticles versus silver ions," *Environmental Science & Technology*, vol. 45, no. 20, pp. 9003–9008, 2011.

[39] R. Y. Prasad, J. K. McGee, M. G. Killius et al., "Investigating oxidative stress and inflammatory responses elicited by silver nanoparticles using high-throughput reporter genes in HepG2 cells: effect of size, surface coating, and intracellular uptake," *Toxicology in Vitro*, vol. 27, no. 6, pp. 2013–2021, 2013.

[40] N. Alissawi, V. Zaporojtchenko, T. Strunskus et al., "Effect of gold alloying on stability of silver nanoparticles and control of silver ion release from vapor-deposited Ag–Au/polytetrafluoroethylene nanocomposites," *Gold Bulletin*, vol. 46, no. 1, pp. 3–11, 2013.

[41] T. Li, B. Albee, M. Alemayehu et al., "Comparative toxicity study of Ag, Au, and Ag–Au bimetallic nanoparticles on *Daphnia magna*," *Analytical and Bioanalytical Chemistry*, vol. 398, no. 2, pp. 689–700, 2010.

[42] S. Grade, J. Eberhard, J. Jakobi, A. Winkel, M. Stiesch, and S. Barcikowski, "Alloying colloidal silver nanoparticles with gold disproportionally controls antibacterial and toxic effects," *Gold Bulletin*, vol. 47, no. 1-2, pp. 83–93, 2013.

[43] C. A. Simpson, K. J. Salleng, D. E. Cliffel, and D. L. Feldheim, "In vivo toxicity, biodistribution, and clearance of glutathione-coated gold nanoparticles," *Nanomedicine: Nanotechnology, Biology, and Medicine*, vol. 9, no. 2, pp. 257–263, 2013.

[44] L. G. Henry, W. Aruni, L. Sandberg, and H. M. Fletcher, "Protective role of the *PG1036-PG1037-PG1038* operon in oxidative stress in *Porphyromonas gingivalis* W83," *PLoS ONE*, vol. 8, no. 8, Article ID e69645, 2013.

[45] Y. Dou, W. Aruni, A. Muthiah, F. Roy, C. Wang, and H. Fletcher, "Studies of the extracytoplasmic function sigma factor PG0162 in *Porphyromonas gingivalis*," *Molecular Oral Microbiology*, 2015.

[46] Y. Dou, D. Osbourne, R. McKenzie, and H. M. Fletcher, "Involvement of extracytoplasmic function sigma factors in virulence regulation in Porphyromonas gingivalis W83," *FEMS Microbiology Letters*, vol. 312, no. 1, pp. 24–32, 2010.

[47] R. M. E. McKenzie, N. A. Johnson, W. Aruni, Y. Dou, G. Masinde, and H. M. Fletcher, "Differential response of *Porphyromonas gingivalis* to varying levels and duration of hydrogen peroxide-induced oxidative stress," *Microbiology*, vol. 158, no. 10, pp. 2465–2479, 2012.

[48] R. M. E. McKenzie, W. Aruni, N. A. Johnson et al., "Metabolome variations in the *Porphyromonas gingivalis vimA* mutant during hydrogen peroxide-induced oxidative stress," *Molecular Oral Microbiology*, vol. 30, no. 2, pp. 111–127, 2015.

[49] L. Kvítek, R. Prucek, A. Panáček, R. Novotný, J. Hrbáč, and R. Zbořil, "The influence of complexing agent concentration on particle size in the process of SERS active silver colloid synthesis," *Journal of Materials Chemistry*, vol. 15, no. 10, pp. 1099–1105, 2005.

[50] L. Kvítek, A. Panáček, J. Soukupová et al., "Effect of surfactants and polymers on stability and antibacterial activity of silver nanoparticles (NPs)," *The Journal of Physical Chemistry C*, vol. 112, no. 15, pp. 5825–5834, 2008.

[51] M. S. Holden, K. E. Nick, M. Hall, J. R. Milligan, Q. Chen, and C. C. Perry, "Synthesis and catalytic activity of pluronic stabilized silver-gold bimetallic nanoparticles," *RSC Advances*, vol. 4, no. 94, pp. 52279–52288, 2014.

[52] D. Paramelle, A. Sadovoy, S. Gorelik, P. Free, J. Hobley, and D. G. Fernig, "A rapid method to estimate the concentration of citrate capped silver nanoparticles from UV-visible light spectra," *Analyst*, vol. 139, no. 19, pp. 4855–4861, 2014.

[53] K. D. Gilroy, A. Sundar, P. Farzinpour, R. A. Hughes, and S. Neretina, "Mechanistic study of substrate-based galvanic replacement reactions," *Nano Research*, vol. 7, no. 3, pp. 365–379, 2014.

[54] X. Xia, Y. Wang, A. Ruditskiy, and Y. Xia, "25th anniversary article: galvanic replacement: a simple and versatile route to hollow nanostructures with tunable and well-controlled properties," *Advanced Materials*, vol. 25, no. 44, pp. 6313–6332, 2013.

[55] E. González, J. Arbiol, and V. F. Puntes, "Carving at the nanoscale: sequential galvanic exchange and Kirkendall growth at room temperature," *Science*, vol. 334, no. 6061, pp. 1377–1380, 2011.

[56] P. Mulvaney, "Surface plasmon spectroscopy of nanosized metal particles," *Langmuir*, vol. 12, no. 3, pp. 788–800, 1996.

[57] G. C. Papavassiliou, "Surface plasmons in small Au-Ag alloy particles," *Journal of Physics F: Metal Physics*, vol. 6, no. 4, pp. L103–L105, 1976.

[58] J. Liu and R. H. Hurt, "Ion release kinetics and particle persistence in aqueous nano-silver colloids," *Environmental Science & Technology*, vol. 44, no. 6, pp. 2169–2175, 2010.

[59] A. Henglein, "Physicochemical properties of small metal particles in solution: 'microelectrode' reactions, chemisorption, composite metal particles, and the atom-to-metal transition," *The Journal of Physical Chemistry*, vol. 97, no. 21, pp. 5457–5471, 1993.

[60] J. C. Love, L. A. Estroff, J. K. Kriebel, R. G. Nuzzo, and G. M. Whitesides, "Self-assembled monolayers of thiolates on metals as a form of nanotechnology," *Chemical Reviews*, vol. 105, no. 4, pp. 1103–1169, 2005.

[61] J. M. Slocik and D. W. Wright, "Biomimetic mineralization of noble metal nanoclusters," *Biomacromolecules*, vol. 4, no. 5, pp. 1135–1141, 2003.

[62] Q. Wu, H. Cao, Q. Luan et al., "Biomolecule-assisted synthesis of water-soluble silver nanoparticles and their biomedical applications," *Inorganic Chemistry*, vol. 47, no. 13, pp. 5882–5888, 2008.

[63] A. Taglietti, Y. A. Diaz Fernandez, E. Amato et al., "Antibacterial activity of glutathione-coated silver nanoparticles against gram positive and gram negative bacteria," *Langmuir*, vol. 28, no. 21, pp. 8140–8148, 2012.

[64] M. Bieri and T. Bürgi, " L-glutathione chemisorption on gold and acid/base induced structural changes: a PM-IRRAS and time-resolved in situ ATR-IR spectroscopic study," *Langmuir*, vol. 21, no. 4, pp. 1354–1363, 2005.

[65] W. Qian and S. Krimm, "Vibrational analysis of glutathione," *Biopolymers*, vol. 34, no. 10, pp. 1377–1394, 1994.

[66] H.-J. Park, J. Y. Kim, J. Kim et al., "Silver-ion-mediated reactive oxygen species generation affecting bactericidal activity," *Water Research*, vol. 43, no. 4, pp. 1027–1032, 2009.

[67] M. A. Kemper, M. M. Urrutia, T. J. Beveridge, A. L. Koch, and R. J. Doyle, "Proton motive force may regulate cell wall-associated enzymes of *Bacillus subtilis*," *Journal of Bacteriology*, vol. 175, no. 17, pp. 5690–5696, 1993.

[68] P. Dibrov, J. Dzioba, K. K. Gosink, and C. C. Häse, "Chemiosmotic mechanism of antimicrobial activity of Ag^+ in *Vibrio cholerae*," *Antimicrobial Agents and Chemotherapy*, vol. 46, no. 8, pp. 2668–2670, 2002.

[69] J. S. Kim, E. Kuk, K. N. Yu et al., "Antimicrobial effects of silver nanoparticles," *Nanomedicine: Nanotechnology, Biology, and Medicine*, vol. 3, no. 1, pp. 95–101, 2007.

[70] M. Yoshimura, Y. Nakano, Y. Yamashita, T. Oho, T. Saito, and T. Koga, "Formation of methyl mercaptan from L-methionine by *Porphyromonas gingivalis*," *Infection and Immunity*, vol. 68, no. 12, pp. 6912–6916, 2000.

[71] L. D. Freedman and A. H. Corwin, "Oxidation reduction potentials of thiol-disulfide systems," *The Journal of Biological Chemistry*, vol. 181, no. 2, pp. 601–621, 1949.